Experimental study on phosphorus distribution ratio and capacity of environment-friendly dephosphorization slag for high-phosphorus hot metal pretreatment

by F. Yang*, X.G. Bi*, and J.D. Zhou*

Synopsis

In this investigation, the phosphorus distribution ratios in the CaF_2 system and B_2O_3 system dephosphorization slags for high-phosphorus hot metal pretreatment were measured by an indirect method under laboratory conditions. Firstly, the phosphorus distribution ratio between liquid slag and solid iron was measured, and then the phosphorus distribution ratio between liquid slag and hot metal was calculated. Phosphorus capacity was calculated in terms of the composition and optical basicity of the slag. Dephosphorization slag was also studied by scanning electron microscopy, energy dispersive analysis, and X-ray diffraction analysis. The experimental results show that the phosphorus capacity of the B_2O_3 slag system is much greater than that of the CaF_2 system. It is demonstrated that B_2O_3 can completely replace CaF_2 as fluxing agent for high-phosphorus hot metal pretreatment. With CaF_2 as fluxing agent, the phosphorus capacity increases with increasing CaO content in the slag, but the phosphorus distribution ratio decreases. B_2O_3, when used as fluxing agent, can react with high melting point phases such as $2CaO \cdot SiO_2$ and $3CaO \cdot P_2O_5$ in the slag to form new phases with low melting points such as $11CaO \cdot B_2O_3 \cdot 4SiO_2$, $2CaO \cdot B_2O_3 \cdot SiO_2$, and $Ca_{9.93}(P_{5.84}B_{0.16}O_{24})$ $(B_{0.67}O_{1.79})$, thereby acting as a fluxing agent. When the ratio of $w(B_2O_3)/w(CaO)$ is 0.16, the phosphorus distribution ratio reaches its maximum value, that is, the dephosphorization ability of the slag is at its maximum.

Keywords

hot metal pretreatment; dephosphorization; phosphorus distribution ratio; phosphorus capacity.

Introduction

As international iron ore prices continue to rise, the development of China's steel industry is facing a lot of pressure. Against this background, development and utilization of domestic high-phosphorus iron ore resources is particularly important. When high-phosphorus iron ore is used in ironmaking, the phosphorus content in the hot metal can reach 0.35% or more, and the hot metal must be pretreated. For hot metal with 0.08–0.10% dissolved phosphorus, the traditional hot metal dephosphorization pretreatment technologies are relatively mature. However, when using these methods to dephosphorize hot metal containing 0.35% P or more, the amount of dephosphorization slag can reach 100–150 kg per ton of hot metal. Furthermore, the traditional dephosphorization methods require

the addition of large amounts of CaF_2 as fluxing agent, and this results in high fluoride levels in the dephosphorization slag. The fluorine in the slag can partially dissolve in water and thereby causes high fluoride concentration in the water and soil. Once the fluoride is absorbed by humans or animals, it can result in toxic effects on the central nervous system and myocardium. In addition, fluoride can accumulate in the environment, and thereby pose a health risk to animals and humans through the food chain (Li, 2007; Liu, Wang, and Dong, 2011, Diao, 2013). The objective of this research is to replace CaF_2 with B_2O_3 as fluxing agent while achieving the expected goals of hot metal pretreatment.

The melting point of B_2O_3 (450°C) is much lower than that of CaF_2 (1419°C). B_2O_3 can interact with FeO, CaO, MgO, and other oxides to form compounds with low melting points such as $CaO \cdot B_2O_3$ (m.p. 1154°C). Compared with CaF_2, B_2O_3 has a greater advantage in rapid slagging (Hamano and Horibe, 2004). The purpose of this article is to investigate the influence of environment-friendly dephosphorizing slag composition on the dephosphorization process, and to provide a theoretical basis for the preparation of an environment-friendly dephosphorization agent that has strong dephosphorization ability. The phosphorus distribution ratio and phosphorus capacity of the CaF_2 slag system were also determined.

Experimental method

The phosphorus distribution ratio and the phosphorus capacity of B_2O_3 dephosphorization slag for high-phosphorus hot metal pretreatment were determined under

* Key Laboratory for Ferrous Metallurgy and Resources Utilization of Ministry of Education, Wuhan University of Science and Technology, Wuhan, China.

Experimental study on phosphorus distribution

laboratory conditions using a thermodynamic equilibrium furnace. The interior structure of the furnace is shown in Figure 1. The compositions of the CaF_2 and B_2O_3 slag systems are shown in Table I and Table II, respectively. The compositions of the pure iron crucible and iron foil are shown in Tables III and IV, respectively. In the experiments, 99.999% high-purity argon gas was purged to provide an inert furnace atmosphere. Slag samples were thoroughly mixed and placed into pure iron crucibles. The crucibles were then loaded into the furnace, and the furnace was heated to 1400°C. The temperature was kept constant for 1 hour, and then lowered to 1350°C, before being kept constant at 1350°C for 11 hours. Finally, the crucibles were removed from the furnace and immediately quenched with water to avoid oxidation reactions that would drive the reactions of Fe_2O_3-FeO-Fe to equilibrium. The pre-melted slag from the equilibrium experiments was crushed, and placed again in pure iron crucibles, together with pure iron flakes of about 1 g weight and 0.1 mm thickness. The crucibles containing the pre-melted slag and iron flakes were then loaded into the furnace, and the temperature was raised to 1300°C and kept constant for 12 hours under argon gas protection to obtain a full equilibrium between the slag and iron flakes. Finally, the crucibles were removed and quenched with water to avoid oxidation that would drive the reaction of P-P_2O_5 to equilibrium. The samples obtained from the experiments were treated as follows.

(1) The slag that had adhered on the iron flakes was ground and cleaned up with supersonic waves in an acetone solution

(2) The phosphorus dissolved in the iron flakes was measured with the molybdenum blue light absorption method. The microstructure and elemental composition of the slag were analysed with scanning electron microscopy using energy-dispersive X-ray spectroscopy (SEM-EDS). The minerals in the slag were characterized by X-ray diffraction.
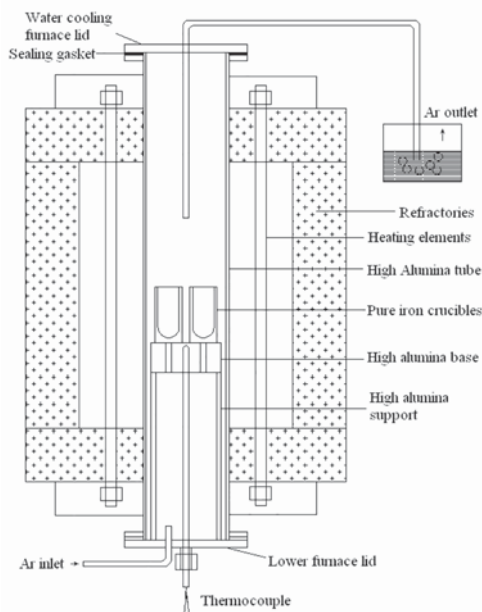

Figure 1—Interior structure of the thermodynamic equilibrium furnace

Calculation of the phosphorus capacity and phosphorus distribution ratio

According to the composition of the slag obtained from the equilibrium experiment, phosphorus capacity is calculated by the following formula (Wei, Yang, and Sommerville, 2002).

$$\lg C_{PO_4^{3-}} = \left(-\frac{36412}{T} + 37\right)\Lambda + \frac{71493}{T} - 30.8 \qquad [1]$$

where $C_{PO_4^{3-}}$ is the phosphorus capacity, T the reaction temperature (K), and Λ the optical basicity. The Λ is the weighted average of the optical basicity of all components in slag, and is calculated using the formula:

$$\Lambda = \sum_{B=1}^{n} x_B \Lambda_B \qquad [2]$$

where Λ_B is the optical basicity of oxide, and x_B is the molar fraction of cations in oxide.

Table I

Composition (mass %) of CaF_2 slag system

No.	FeO	SiO_2	P_2O_5	CaO	CaF_2
1-0-1	11.32	7.06	13.44	51.73	16.45
1-0-2	10.24	9.12	16.12	48.75	15.77
1-0-3	10.50	10.79	18.50	46.10	14.31
1-0-4	10.37	12.03	19.65	43.72	14.23

Table II

Composition (mass %) of B_2O_3 slag system

No.	$w(B_2O_3)/w(CaO)$	FeO	SiO_2	P_2O_5	CaO	B_2O_3
3-0-1	0.08	8.14	9.93	15.28	61.71	4.94
3-0-2	0.10	5.37	9.71	15.78	62.85	6.29
3-0-3	0.12	5.85	9.81	15.43	61.53	7.38
3-0-4	0.14	6.66	7.24	15.41	62.01	8.68
3-0-5	0.16	6.34	7.30	14.65	61.82	9.89
3-0-6	0.18	5.68	7.15	14.36	61.79	11.12

Table III

Composition of pure iron crucible (mass %)

C	Si	P	Mn	S	N
0.008	0.002	0.006	0.017	0.005	0.008

Table IV

Composition of iron foil (mass %)

C	Si	Mn	P	S	Cr	Cu
0.07	0.0032	0.036	0.021	0.001	0.006	0.032
Ti	V	As	B	Zn	Fe	
0.0012	0.0001	0.005	0.001	0.011	99.8	

Experimental study on phosphorus distribution

x_B also denotes the molar fraction of oxygen of oxide in the slag, and is calculated by formula:

$$x_B = \frac{n_O x_B'}{\sum n_O x_B'} \qquad [3]$$

where x_B' is molar fraction of oxide, n_O is the number of oxygen atoms in the oxide molecule. It is specified that one fluorine atom in the fluoride molecule is equal to 1/2 oxygen atoms. x_B' can be calculated by:

$$x_B' = \frac{w_B / M_B}{\sum \frac{w_B}{M_B}} \qquad [4]$$

where w_B is the percentage of oxide and M_B is the molar mass of oxide.

In this paper, the measured value of the phosphorus distribution ratio is not between liquid slag and carbon-saturated hot metal but between liquid slag and solid iron flake, thus a conversion is needed. Im, Morita, and Sano (1996) calculated the phosphorus distribution ratio between liquid slag and solid pure iron flakes (Tsukihashi, Nakamura, and Orimoto, 1990; Knacke, Kubaschewski, and Heselmann, 1991; Im, Morita, and Sano, 1996; Zhou *et al.*, 2011). The expression of phosphorus distribution ratio is as follows:

$$L_P^{Fe-\alpha,\gamma} = \frac{(\%P)}{[\%P]^{Fe-\alpha,\gamma}} \qquad [5]$$

where $\alpha L_P^{Fe-\alpha}$ is the phosphorus distribution ratio between liquid slag and α iron, $L_P^{Fe-\gamma}$ the phosphorus distribution ratio between liquid slag and γ iron, %P the mass percentage of P in liquid slag, $[\%P]^{Fe-\alpha}$ the mass percentage of P in α iron, and $[\%P]^{Fe-\gamma}$ is the mass percentage of P in γ iron.

After thermodynamic conversion, the distribution of phosphorus between carbon-saturated iron and α iron and γ iron is obtained by:

$$\frac{[\%P]^{Fe-a}}{[\%P]^{Fe-C}} = 0.779 \qquad [6]$$

([P] in solid iron is larger than 0.41%)

$$\frac{[\%P]^{Fe-\gamma}}{[\%P]^{Fe-C}} = 0.413 \qquad [7]$$

([P] in solid iron is smaller than 0.41%)

where $[\% P]^{Fe-C}$ is the mass percentage of P in carbon-saturated hot metal.

Results and discussion

Phosphorus capacity and phosphorus distribution ratio of CaF$_2$ slag system

Equilibrium compositions and phosphorus capacity calculated for the CaF$_2$ slag system are shown in Table V.

The phosphorus contents in the CaF$_2$ slag system and solid iron flake, and the phosphorus distribution ratio between liquid slag and carbon-saturated hot metal are also shown in Table VI. The relationship between phosphorus distribution ratio and CaO content is depicted in Figure 2.

It can be clearly seen from Table V that when the CaO content in the slag is the highest, the phosphorus capacity of the CaF$_2$ slag system reaches the maximum value. That is, at a CaO content in slag of 49.72%, the phosphorus capacity is 11.66×10^{22}. At a CaO content in slag of about 44%, the change in phosphorus capacity is small. As can be seen from
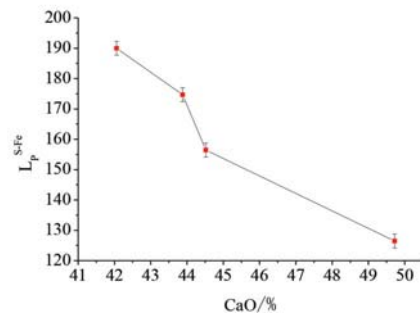

Figure 2—Relationship between phosphorus distribution ratio and CaO content

Table V

Equilibrium composition (mass %) and phosphorus capacity of CaF$_2$ slag system

Test number	FeO	Fe$_2$O$_3$	CaO	SiO$_2$	P	CaF$_2$	$C_{PO_4^{3-}}$ x 10^{22}
1-0-1	7.64	3.2	49.72	6.91	5.39	16.06	11.66
1-0-2	5.63	3.14	44.52	8.99	6.44	15.12	3.274
1-0-3	5.78	2.3	43.88	10.51	7.19	14.60	2.948
1-0-4	6.52	2.86	42.06	11.72	8.28	13.61	2.331

Table VI

Phosphorus distribution ratio of CaF$_2$ slag system

Test number	(FeO) (mass %)	(P) (mass %)	[P]$_{Fe}$ (mass %)	LP^{s-Fe}
1-0-1	7.64	5.39	0.0176	126.48
1-0-2	9.63	6.44	0.0172	156.45
1-0-3	5.78	7.19	0.0176	174.67
1-0-4	6.52	8.28	0.0179	189.98

Experimental study on phosphorus distribution

Table VI and Figure 2, $L_p^{\text{s-Fe}}$ increases with decreasing CaO content. For example, as the CaO content decreases from 49.72% to 42.06%, the $L_p^{\text{s-Fe}}$ increases from 126.84 to 189.98. $L_p^{\text{s-Fe}}$ is influenced synthetically by slag basicity, fluxing agent content (effect of slag melting), and FeO content, among other factors. $L_p^{\text{s-Fe}}$ of the slag in test 1-0-4 is 189.98, the maximum value. The basicity of 1-0-4 slag is 3.76. However, $L_p^{\text{s-Fe}}$ of 1-0-1 slag reaches the minimum value, with a basicity of 17.20. When the basicity is too high, the dephosphorizing slag contains solid CaO particles deposited from the bath. The higher the basicity, the more CaO particles are deposited. Figures 3 and 4 show elemental analyses and a micrograph of CaO solid particles in melted slags from tests 1-0-2 and 1-0-3, respectively. It can be clearly seen that the quantity and size of CaO particles in melted slag with 44.52% CaO are much greater than in slag with 43.88% CaO. This explains why $L_p^{\text{s-Fe}}$ bears an inverse relationship to CaO content. More CaO particles increase the viscosity of slag, which in turn decreases $L_p^{\text{s-Fe}}$. In this condition, it is required to decrease the basicity of the slag, increase the amount of fluxing agent, or increase the FeO content of the slag.

Phosphorus capacity and phosphorus distribution ratio of B_2O_3 slag system

Equilibrium compositions and phosphorus capacity calculated for the B_2O_3 slag system are shown in Table VII.

Phosphorus distribution ratios obtained for the B_2O_3 slag system between liquid slag and carbon-saturated hot metal are shown in Table VIII. The relationship between phosphorus distribution ratio and $w(B_2O_3)/w(CaO)$ is depicted in Figure 5.

As can be seen from Table VII, the phosphorus capacity of all B_2O_3 slag system is generally higher. The highest value is as high as 57.54×10^{23}. It can be seen from Table VIII and Figure 5 that at a $w(B_2O_3)$ to $w(CaO)$ ratio of 0.16, the phosphorus distribution ratio reaches the highest value of 156.12. As the B_2O_3 content continues to increase, the phosphorus distribution ratio begins to decrease. As such, this kind of slag system (test number 3-0-5) has the highest dephosphorization ability.

When the quantity of B_2O_3 is appropriate, during the dephosphorization reaction, B_2O_3 reacts with $2CaO \cdot SiO_2$ to form $11CaO \cdot B_2O_3 \cdot 4SiO_2$ and $2CaO \cdot B_2O_3 \cdot SiO_2$. Moreover, B_2O_3
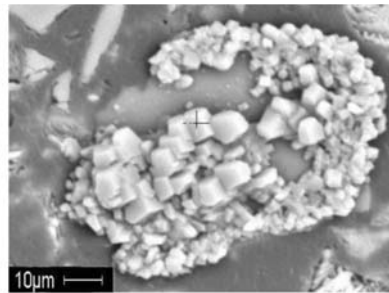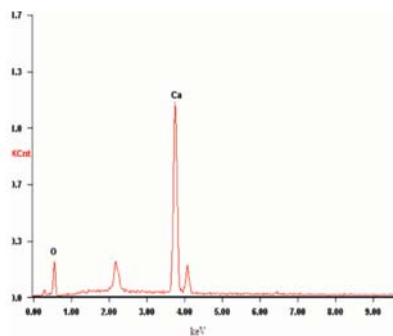

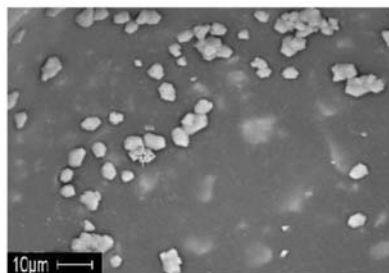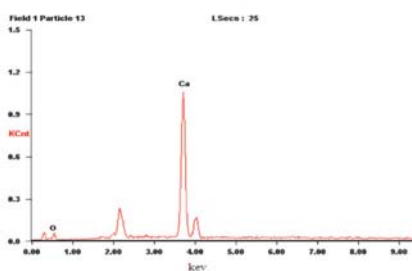**Figure 3—Elemental analysis and micrograph of CaO particles in slag, test 1-0-2**

Figure 4—Elemental analysis and micrograph of CaO particles in slag, test 1-0-3

Table VII

Equilibrium composition (mass %) and phosphorus capacity of CaF$_2$ slag system

Test number	$w(B_2O_3)/w(CaO)$	FeO	Fe$_2$O$_3$	CaO	SiO$_2$	P	B$_2$O$_3$	$C_{PO_4^{3-}} \times 10^{23}$
3-0-1	0.08	6.55	1.58	60.91	8.23	4.83	4.87	6.46
3-0-2	0.10	4.15	1.30	60.86	5.62	5.79	6.47	57.54
3-0-3	0.12	5.58	1.13	59.41	8.29	5.69	7.02	2.95
3-0-4	0.14	4.54	2.76	60.81	5.53	5.63	8.12	5.62
3-0-5	0.16	5.30	1.39	59.58	8.26	6.88	9.48	1.41
3-0-6	0.18	4.54	1.43	60.85	5.40	5.68	10.95	3.09

Experimental study on phosphorus distribution

Table VIII

Phosphorus distribution ratios of B_2O_3 slag system

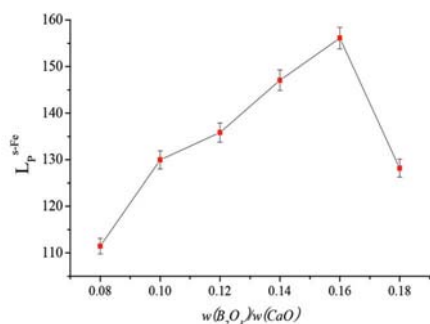| Test number	(FeO) (mass %)	(P) (mass %)	$[P]_{Fe}$ (mass %)	$LP^{s\text{-}Fe}$
3-0-1	6.55	4.83	0.0179	111.44
3-0-2	4.15	5.79	0.0184	129.96
3-0-3	5.58	5.69	0.0173	135.83
3-0-4	4.54	5.63	0.0183	147.06
3-0-5	5.30	6.88	0.0182	156.12
3-0-6	4.54	5.68	0.0183	128.19

Figure 6—XRD pattern of $w(B_2O_3)/w(CaO)=0.164$

Figure 5—Relationship between phosphorus distribution ratio and $w(B_2O_3)/w(CaO)$

continues to react with $3CaO \cdot P_2O_5$, which is formed by reaction between CaO and P_2O_5, to form $Ca_{9.93}(P_{5.84} B_{0.16}O_{24})$ $(B_{0.67}O_{1.79})$, which has a low melting point. Thus B_2O_3 acts as a fluxing agent and is beneficial for dephosphorization reactions. In this case, the phosphorus distribution ratio and capacity are the highest. The XRD pattern from test 3-0-5 is shown in Figure 6.

Conclusions

With CaF_2 as fluxing agent, the phosphorus capacity of dephosphorization slag for high-phosphorus hot metal is between 2.331×10^{22} and 11.66×10^{22}. Phosphorus capacity increases with increasing slag basicity. However, too high a CaO content adversely affects the phosphorus distribution ratio because the melting of the dephosphorization slag becomes difficult, and this reduces the fluidity of the slag, hindering diffusion and decreasing the dephosphorization rate.

The phosphorus capacity of the B_2O_3 slag system is between 1.41×10^{23} and 57.54×10^{23}, which is one order of magnitude higher than CaF_2 system. It has been demonstrated that B_2O_3 can completely replace CaF_2 as fluxing agent for high-phosphorus hot metal pretreatment.

The phosphorus distribution ratio of the B_2O_3 system is 111.44–156.12. At a $w(B_2O_3)$ to $w(CaO)$ ratio of 0.16, the phosphorus distribution ratio reaches its highest value. The dephosphorization ability of this slag system is therefore the strongest.
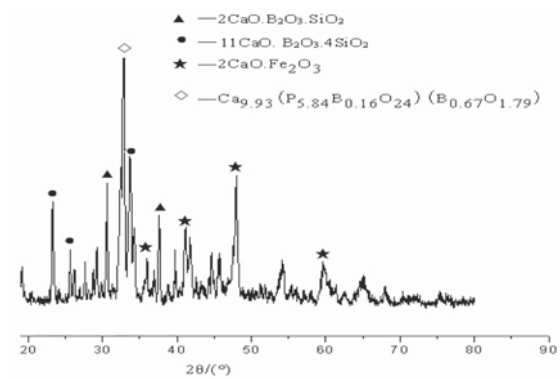
References

Diao, J. 2013. Effect of Al_2O_3 and Na_2O on dephosphorization of high phosphorus hot metal. *Journal of Iron and Steel Research*, vol. 25, no. 2. pp. 9–10.

Hamano, T. and Horibe, M. 2004. The dissolution rate of solid lime into molten slag used for hot-metal dephosphorization. *ISIJ International*, vol. 44, no. 2. pp. 263–267.

Im, J., Morita, K., and Sano, N. 1996. Phosphorus distribution ratios between CaO-SiO_2-Fe_tO slags and carbon-saturated iron at 1573K. *ISIJ International*, vol. 36, no. 5. pp. 517–521.

Li, C. 2007. Fluoride pollution sources, control technology and its source. *Iron & Steel Technology*, no. 3. pp. 5–153.

Knacke, O., Kubaschewski, O., and Heselmann, K. 1991. Thermochemical Properties of Inorganic Substance. Springer-Verlag, Berlin.

Liu, L., Wang, S., and Dong, Y. 2011. Performance of low fluoride dephosphorization slag of hot metal. *Journal of Iron and Steel Research International*, vol. 18, no. 1. pp. 11–15.

Tsukihashi, F., Nakamura, M., and Orimoto, T. 1990. Thermodynamics of phosphorus for the CaO-$FetO$-CaF_2-SiO_2 and CaO-Al_2O_3 systems. *Tetsu-to Hagane*, vol. 76, no. 10. pp. 1664–1671.

Wei, E. Yang, Y., and Sommerville, I.D. 2002. The fundamentals of using custom-designed slags to remove impurities from liquid steel. *Proceedings of the 60th Electric Furnace Conference*, San Antonio, TX, 10–13 November 2002. Kanagy, D.L. and Baker, M.A. (eds.). Iron & Steel Society, Warrendale, PA. pp. 761–771.

Zhou, J. Bi , X, Huang, Z., and Jin, Y. 2011. Phosphorus distribution equilibrium between CaO-FeO^*-SiO_2-P_2O_5(15%)-CaF_2(B_2O_3) slag system and carbon-saturated hot metal at 1573K. *Proceedings of the International Conference on Chemical, Material and Metallurgical Engineering*, Beihai, China 23-25 December, 2011. Trans Tech Publications, Zurich. pp. 369–372. ◆